

시간영역 수동제어기의 미세떨림현상 제거

Removing the Noisy Behavior of the Time Domain Passivity Controller

유 지 환*
(Jee-Hwan Ryu)

Abstract : A noisy behavior of the time domain passivity controller during the period of low velocity is analyzed. Main reasons of the noisy behavior are investigated through a simulation with a one-DOF (Degree of Freedom) haptic interface model. It is shown that the PO/PC is ineffective in dissipating the produced energy when the sign of the velocity, which is numerically calculated from the measured position, is suddenly changed, and when this velocity is zero. These cases happen during the period of low velocity due to the limited resolution of the position sensor. New methods, ignoring the produced energy from the velocity sign change, and holding the control force while the velocity is zero, are proposed for removing the noisy behavior. The feasibility of the developed methods is proved with both a simulation and a real experiment.

Keywords : noisy behavior, haptic interface, passivity controller, passivity observer, time-domain passivity

I. Introduction

A haptic interface is a kinesthetic link between a human operator and a virtual environment (VE). One of the most significant problems in haptic interface design is to create a control system which simultaneously is stable (i.e. does not exhibit vibration or divergent behavior) and gives high fidelity under any operating conditions and for any virtual environment parameters. There are several mechanisms by which a virtual environment or other part of the system might exhibit active behavior. These include quantization [4], interactions between the discrete time system and the continuous time device/human operator [5], and delays due to numerical integration schemes [14].

Initial efforts to solve this problem introduced the “virtual coupling” between the virtual environment and the haptic device [1,4,22]. The virtual coupling parameters can be set empirically, but several previous research projects have sought out a theoretical design procedure using control theory. However, interesting virtual environments are always non-linear and the dynamic properties of a human operator are always involved. These factors make it difficult to analyze haptic systems in terms of system models with known parameters and linear control theory. Anderson and Spong [2] and Neimeyer and Slotine [15] have used passivity ideas in the related area of stable control of force-feedback teleoperation with time delay. Colgate and Schenkel [5] have used it to derive fixed parameter virtual couplings (i.e., haptic interface controllers). The major problem with using passivity for design of haptic interaction systems is that it is over conservative. In many cases performance can be poor if a fixed damping value is used to guarantee passivity under all operating conditions. Several other passivity based approaches were also proposed for stable haptic interaction [3,10,11].

A different passivity based approach has been proposed by

Hannaford and Ryu [6], that measures active system behavior and injects variable damping whenever net energy is produced by the virtual environment. They proposed a “Passivity Observer” (PO) and a “Passivity Controller” (PC) to insure stable contact under a wide variety of operating conditions. Recently, the PO/PC approach has been improved for estimating exact energy output [17], and removing sudden impulsive PC force [18].

In our previous researches [6,16-18], the PO/PC was ineffective in dissipating the produced energy during the period of low velocity (series type PC in impedance causality) or low force (parallel type PC in admittance causality), and it has been open as a future work. We have named this undesirable behavior as a “noisy behavior” due to the unwanted high frequency oscillations of position and force. Even though there has been an effort to solve the noise problem [8], it was a tuning method of heuristic control parameters depending on a system. In this paper, main reasons of the noisy behavior of the PO/PC are analyzed, and methods to remove the noisy behavior are proposed.

II. Review of the Time Domain Passivity Approach

In this section, we briefly review time-domain passivity control. First, we define the sign convention for all forces and velocities so that their product is positive when power enters the system port (Fig. 1). Also, the system is assumed to have initial stored energy $E(0)=0$ at $t = 0$. The following widely known definition of passivity is used.

Definition 1: The one-port network, N, with initial energy storage $E(0)=0$ is passive if and only if,

$$\int_0^t f(\tau)\dot{x}(\tau)d\tau \geq 0, \quad \forall t \geq 0 \quad (1)$$

holds for admissible forces (f) and velocities (\dot{x}). Eqn (1) states that the energy supplied to a passive network must be positive for all time [20,21].

The elements of a typical haptic interface system include the virtual environment, the virtual coupling network, the haptic device controller, the haptic device, and the human operator.

* 책임저자(Corresponding Author)

논문접수 : 2005. 6. 9, 채택확정 : 2005. 12. 14.

유지환 : 한국기술교육대학교 기계정보공학부(jhryu@kut.ac.kr)

※ 본 논문은 한국기술교육대학교 신입교수연구과제(2006년) 및 산자부 지역혁신특성화사업(CAERIS, RIS-05-004)에 의하여 지원되었음.

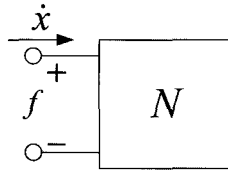


그림 1. 원포트 네트워크.
Fig. 1. One-port network.

Many of the input and output variables of these elements of haptic interface systems can be measured by the computer and (1) can be computed in real time by appropriate software. This software is very simple in principle because at each time step, (1) can be evaluated with few mathematical operations.

The conjugate variables that define power flow in such a system are discrete-time values, and the analysis is confined to systems having a sampling rate substantially faster than the dynamics of the system. We assumed that there is no change in

force and velocity during one sample time. Thus, we can easily “instrument” one or more blocks in the system with the following “Passivity Observer,” (PO) for a one-port network to check the passivity (1).

$$E_{obsv}(k) = \Delta T \sum_{j=0}^k f(t_j)v(t_j) \quad (2)$$

where ΔT is the sampling period, and $t_j = j \times \Delta T$. If $E_{obsv}(k) \geq 0$ for every k , this means the system does not generate energy. If there is an instance when $E_{obsv}(k) < 0$, this means the system generates energy and the amount of generated energy is $-E_{obsv}(k)$. Other research has allowed this constant force and velocity assumption to be relaxed [17,19], and, in [17], the more accurate PO, which predict one-step ahead energy input, was proposed.

Consider a one-port system which may be active. Depending on operating conditions and the specifics of the one-port element's dynamics, the PO may or may not be negative at a particular time. However, if it is negative at any time, we know that the one-port may then be contributing to instability. Moreover, since we know the exact amount of energy generated, we can design a time-varying element to dissipate only the required amount of energy. We call this element a “Passivity Controller” (PC). The PC takes the form of a dissipative element in a series or parallel configuration depending on the input causality [6].

Recently, reference energy following method was proposed [18] for removing sudden impulsive force of the PC with the following time-varying energy threshold instead of fixed zero energy threshold as follows:

$$W(k) = \sum_{j=0}^k f(t_{j-1})(x(t_j) - x(t_{j-1})) \geq E_{ref}(t_k), \forall t_k \geq 0, \quad (3)$$

where $W(k)$ is the PO value for the case of impedance causality, which is the net energy input to a one-port network from 0 to t_k , and $E_{ref}(t_k)$ is the time-varying reference energy threshold which can be designed using VE model

information or conjugate pair of input/output signal.

Please refer to [6,16-18] for more detail about time domain passivity control approach.

III. Analysis of the Noisy Behavior of the PO/PC

In this Section, the main reasons of the noisy behavior are investigated through the simulation of a one-DOF haptic interface system (Fig. 2), consists of the Human Operator (HO), the Haptic Interface (HI), the PC, and the VE with impedance causality. Electrical circuit representation is used between HO and HI since the causality is hard to be defined at this kind of physical interaction port, and input-output representation is used between HI and VE because this is a user defined signal port. There were well known researches about human dynamics in man-machine systems [12,13]. However, in this paper, human and device are assumed to be one-DOF linear time invariant models as used in many other researches [1,5,6] for making the problem as simple as possible. The following simulation parameters were used for HO and HI.

$$M_{HO} = 0.1(Kg), B_{HO} = 0.5(Ns/m), K_{HO} = 50(N/m),$$

$$M_{HI} = 0.2(Kg), B_{HI} = 0.0(Ns/m), K_{HI} = 0.0(N/m).$$

Note that the HI and HO have very low damping, and the high stiffness VE consists of a first order, penalty based spring model ($K = 1000 N/m$) executed at 1000 Hz. Two separate simulations with 1.0×10^5 Hz, one in Matlab/simulink, and one in a C program using trapezoidal integration were used including sensor quantization effect (minimum resolution is $1.0 \times 10^{-5} (m)$). The most recent PO/PC approach, which makes the energy input follows the desired reference energy behavior [18], was used at 1000 Hz.

The HI was pushed to make a contact with the high stiffness VE at Position ≥ 0 . The contact seemed stable (Fig. 3a) on the position response, but the PC input was chattering (Fig. 3d) and the PO value kept falling down to more negative value (Fig. 3c) during the period of low velocity. As a result, operator felt small and continuous vibration. Note that we bounded the PC force to escape the sudden big force change.

Fig. 4 shows the one-step backward velocity $\left(v(k) = \frac{x(t_k) - x(t_{k-1})}{\Delta T} \right)$ of the above simulation. One-step backward velocity is the most appropriate velocity notation for explaining the effect of the velocity to the PO value (3). When the velocity was converged to the minimum resolutions ($\pm 1.0 \times 10^{-2} m/s$), it started chattering with high frequency.

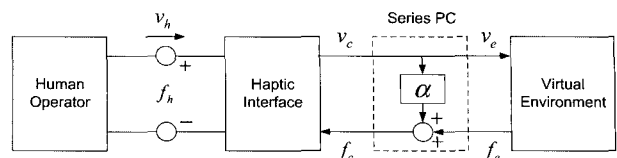


그림 2. 시리즈 PC를 포함한 햅틱인터페이스 시뮬레이션 모델.
Fig. 2. Haptic interface system with series type PC for simulation.

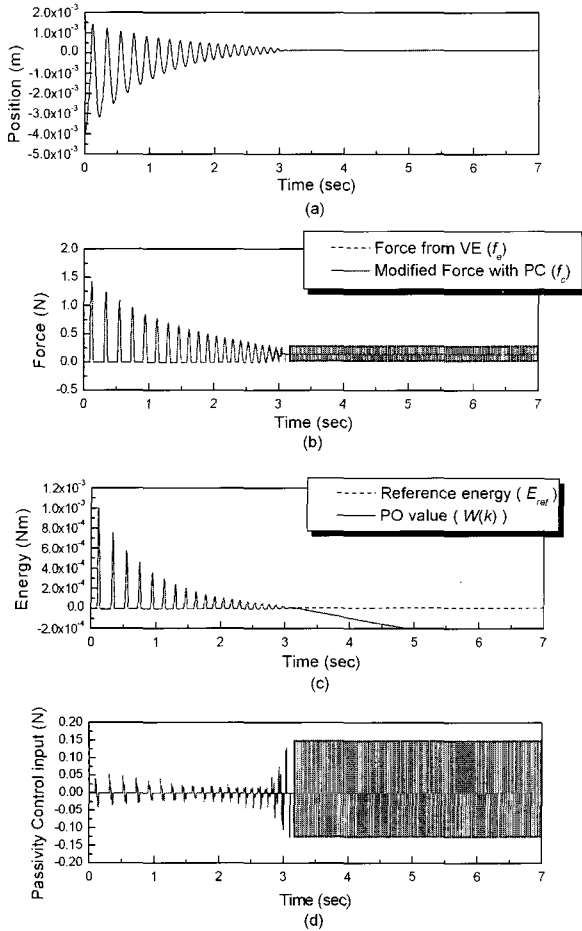


그림 3. 에너지 추종 PO/PC를 사용할 때 강성이 높은 가상환경($K = 1000 \text{ N/m}$)과 접촉시의 반응. 속도가 낮은 구간에서 PC에 잡음이 있다.

Fig. 3. Contact response with the energy following PO/PC [18] for the high stiffness VE ($K = 1000 \text{ N/m}$). PC was noisy during the period of low velocity.

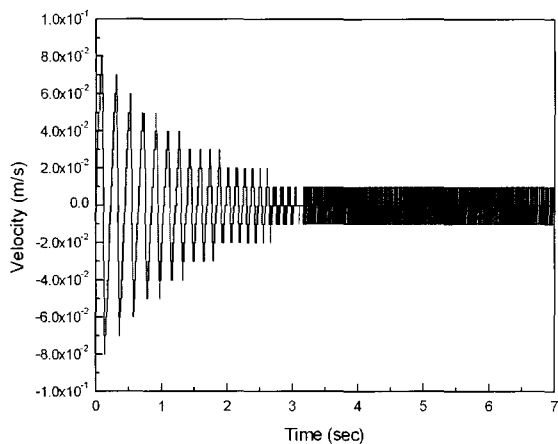


그림 4. 상호작용 시 수치적으로 계산된 백워드 속도. 시간이 2.5초 이상일 때 속도는 최저 값에서 진동하고 있다.

Fig. 4. The numerical backward velocity during the interaction. Velocity was chattering between minimum resolutions when $t_k > 2.5 \text{ sec}$.

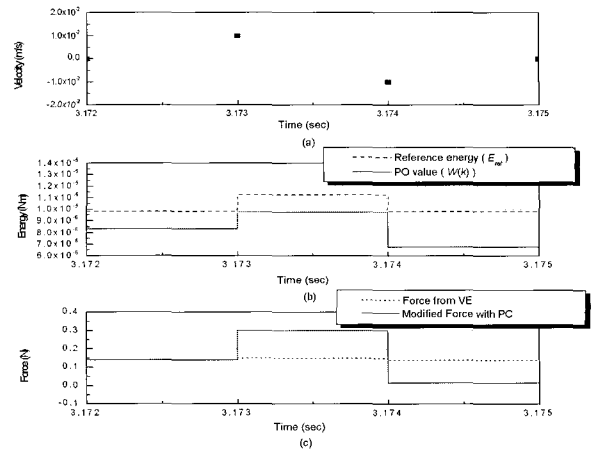


그림 5. 갑작스런 속도의 변화와 그에 의한 PO값의 변화.

Fig. 5. Sudden sign change of the velocity and its effect to the PO value.

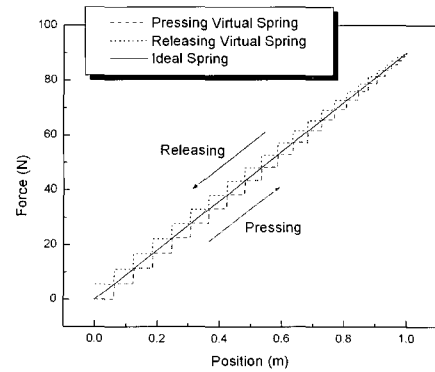


그림 6. 가상 스프링의 변위에 따른 힘의 변화.

Fig. 6. Position vs. force response of a virtual spring.

There are two undesirable behaviors of the velocity which make the PO/PC ineffective due to the limited resolution of the position sensor.

1. Sudden Sign Change of the Velocity

When the sign of the numerical velocity is suddenly changed from positive (or negative) at step k to negative (or positive) at step $k+1$, the energy difference between the PO value and the reference energy is increased even with the PC force. Fig. 5 shows the magnified velocity and energy behavior of the above simulation. When the sign of the velocity was positive at $t=3.173 \text{ (sec)}$ (Fig. 5a), the PC increased the output force (Fig. 5c) to reduce the energy difference (Fig. 5b). However the energy difference was increased when the velocity became negative at $t=3.174 \text{ (sec)}$ since the PO update rule is like

$$W(k+1) = W(k) + f_c(k)v(k+1)\Delta T. \quad (4)$$

This undesirable behavior can be explained with position versus force response of a VE as well. Before we explain the main idea, it is worth while to remind the example in our previous paper [17]. We have shown position versus force response of a VE which composed of a linear spring (Fig. 6).

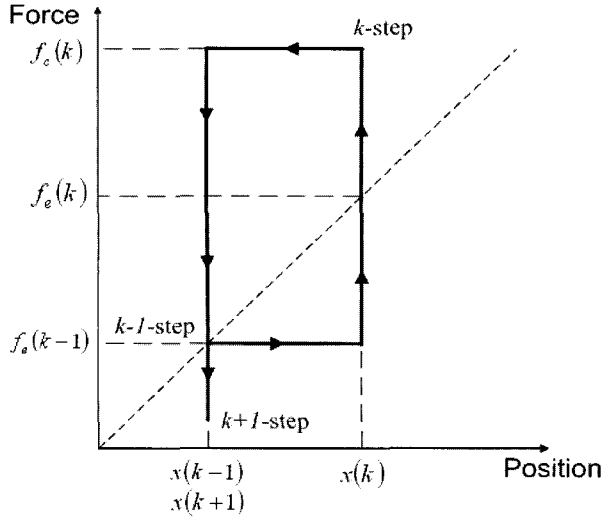


그림 7. 속도의 부호가 한 샘플타임 후에 변할 때 변위에 따른 힘의 변화.

Fig. 7. Position vs. force response when the velocity sign is changed in one sample time.

It has shown a staircase shape due to the discrete-time sampling, the limited resolution of the position sensor and the Zero Order Holder (ZOH). The solid line indicates the behavior of the ideal linear spring. The dashed line shows the case when the VE is pressed, and the dotted line shows the case when the VE is released. The area below each curve is the amount of energy that is dissipated and produced during the pressing and releasing process, respectively. The VE dissipates less energy, and produces more energy compared to the ideal spring. Thus, the VE is active while the ideal spring is passive. In [18], the PC was activated to shift up the dashed line and shift down the dotted line for making the net energy of the VE following the energy behavior of the ideal spring.

The measured position versus force response with PC is magnified for the case when the sign of the velocity is changed in one sample time (Fig. 7). Assume that the measured position was increased from $x(k-1)$ to $x(k)$ at step k , and back to the initial value at step $k+1$. If both the PO and the reference energy had the same value ($E(k-1)$) at step $k-1$, each values at step k would be as follows:

$$\begin{aligned} W(k) &= E(k-1) + f_e(k-1)(x(k) - x(k-1)), \\ E_{ref}(k) &= E(k-1) + f_e(k-1)(x(k) - x(k-1)) \\ &\quad + \frac{1}{2}(f_e(k) - f_e(k-1))(x(k) - x(k-1)), \end{aligned}$$

where the amount of increment is the area below each curve. Since the PO value was less than the reference energy, the PC was activated to make the PO value follows the reference energy based on the current positive velocity. As a result, the force output was increased from $f_e(k)$ to $f_e(k) + f_{pc}(k)$, where $f_{pc}(k)$ is the passivity control input. However, the energy difference between the PO value and the reference energy was even increased at step $k+1$ since the sign of the velocity was suddenly changed.

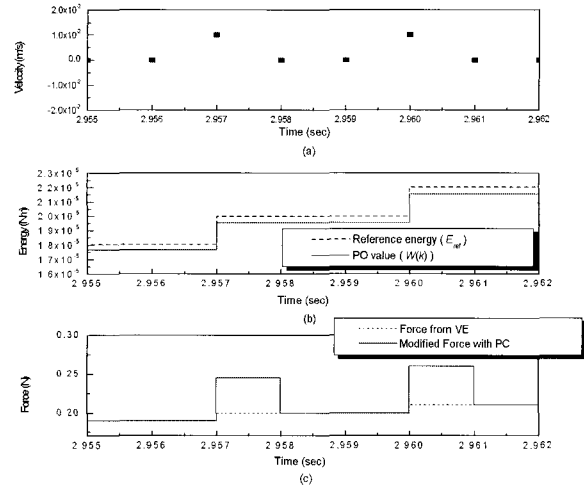


그림 8. PC동작 후 속도가 0이 된 경우, PO값에 미치는 영향.
Fig. 8. Zero velocity after the PC action and its effect to the PO value.

$$\begin{aligned} W(k+1) &= E(k-1) + f_e(k-1)(x(k) - x(k-1)) + f_e(k)(x(k+1) - x(k)) \\ &= E(k-1) + (f_e(k-1) - f_e(k))(x(k) - x(k-1)) \\ E_{ref}(k+1) &= E(k-1) + f_e(k-1)(x(k) - x(k-1)) \\ &\quad + \frac{1}{2}(f_e(k) - f_e(k-1))(x(k) - x(k-1)) \\ &\quad + f_e(k-1)(x(k+1) - x(k)) \\ &\quad + \frac{1}{2}(f_e(k) - f_e(k-1))(x(k+1) - x(k)) \\ &= E(k-1). \end{aligned}$$

With this velocity change, certain amount of energy $((f_e(k) - f_e(k-1))(x(k) - x(k-1)))$ was produced while the reference energy got back to the initial value. If the same situation happens several times, the energy difference become bigger, and the magnitude of the PC input will be increased.

2. Zero Values of the Velocity

Even though the sudden sign change of the velocity increased the energy difference between the PO value and the reference energy, the PC is supposed to make up for the energy difference for the rest of the cases. However, the PC could not give any effect for compensating the energy difference during the period of low velocity since the numerically calculated velocity were zero for the most of the time due to the resolution of the position sensor.

Fig. 8 shows the case by magnifying the above simulation result (Fig. 3). Even though the PC was activated at $t=2.957(\text{sec})$ (Fig. 8c) and increased the output force, the energy difference at the next step ($t=2.958(\text{sec})$) was not changed (Fig. 8b) due to the zero velocity at $t=2.958(\text{sec})$ (Fig. 8a).

Assume that the velocity at step k was positive, and zero at step $k+1$ (Fig. 9). The PO values at step k and $k+1$ would be

$$\begin{aligned} W(k) &= E(k-1) + f_e(k-1)(x(k) - x(k-1)), \\ W(k+1) &= E(k-1) + f_e(k-1)(x(k) - x(k-1)) + f_e(k)(x(k+1) - x(k)) \\ &= E(k-1) + f_e(k)(x(k+1) - x(k)). \end{aligned}$$

Even though the PC was activated at step k to make the PO follow the reference energy, the PC could not give any effect to the PO value at step $k+1$ since there was no position displacement ($x_k = x_{k+1}$). Therefore, the PC even makes the performance feel worse without any energy modification.

IV. Method for Removing the Noisy Behavior

Through the deep analysis, we found two main reasons of the noisy behavior during the period of the low velocity. The first one was the sudden sign change of the numerically calculated velocity in one sample time, and the second one was the zero value of the velocity after the PC action. In this Section, methods to remove the noisy behavior are proposed based on the above analysis.

The first idea we could apply for solving this noisy behavior is estimating the velocity. A starting point of the velocity/displacement estimation was in [9]. Relatively nonconservative velocity filter in [7] was used for the same simulation of Fig. 3. However, the results were much worse in Fig.10. The estimation error from the delay of the filter made the PO value, based on the filtered velocity, greater than the reference energy (Fig. 10b). Therefore the PC was not activated (Fig. 10d) even though the system was vibrating (Fig. 10a).

Followings are two respective methods for removing undesirable behaviors which were introduced in Section III.

1. Ignoring the Produced Energy from the Velocity Sign Change

Fig. 11 shows the measured position and the actual position of the simulation (in Fig. 3) during the period of low velocity. In the simulation, quantization effect was considered as follows:

$$\begin{aligned} & \text{If } x_1 - \Delta x \leq x(t_k) < x_1 \text{ then } x(k) = x_1 - \Delta x, \\ & \text{elseif } x_1 \leq x(t_k) < x_1 + \Delta x \text{ then } x(k) = x_1, \end{aligned}$$

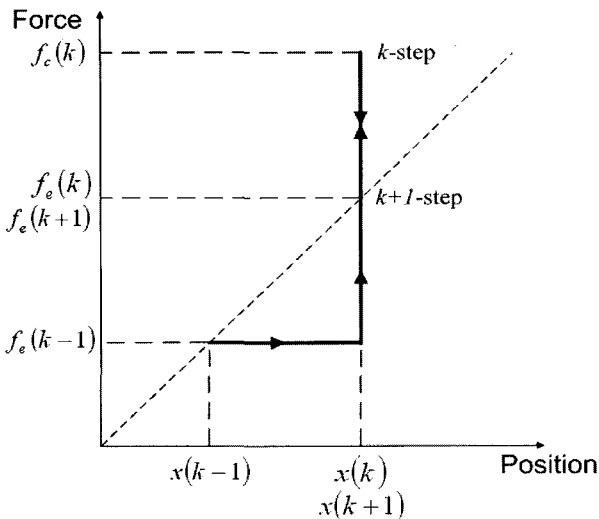


그림 9. PC동작 후 속도가 0이 된 경우, 변위에 따른 힘의 변화.

Fig. 9. Position vs. force response when the velocity become zero after the PC action.

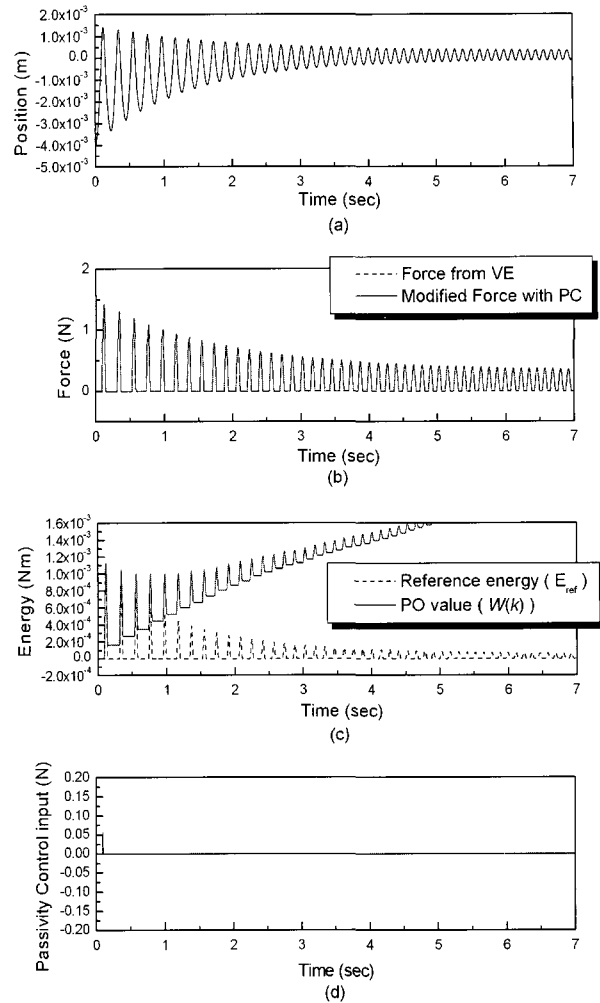


그림 10. 필터링 된 속도에 기반한 에너지 추종 PO/PC의 응답. 안정적이지 못함에도 불구하고 PO값이 기준 값보다 항상 크다.

Fig. 10. Contact response with the energy following PO/PC, based on filtered velocity, for the high stiffness VE ($K = 1000 \text{ N/m}$). The PO value was greater than the reference energy value even though the contact was unstable.

where Δx is the minimum resolution of the position sensor, and x_1 is an integer multiple of Δx . The actual position was varying while the measured position was staying constant, and the small displacement near digitized line caused discrete change of the measured position. If the actual position behavior is considered for the calculation of the PO, the more accurate and nonconservative PO value can be obtained for escaping the unnecessary PC operation.

Based on the observation in Fig. 11, the actual position versus force response is redrawn when the sign of the velocity is suddenly changed in one sample time (Fig. 12). Since we confined the analysis to systems that have fast enough sampling rate compared to the system mode, the width of the rectangle in Fig. 12 is closer to zero than it is to the rectangle in Fig. 7, so it is better to ignore it rather than include a rectangle like Fig. 7.

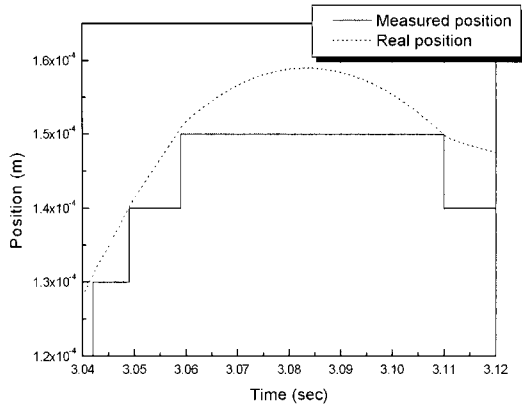


그림 11. 저속구간에서 실제변위와 측정된 변위의 비교. 측정값이 고정되어 있을 때에도 실제 값은 지속적으로 변한다.

Fig. 11. Comparison of the actual position vs. measured position during the period of low velocity. The actual position was varying while the measured position remained constant.

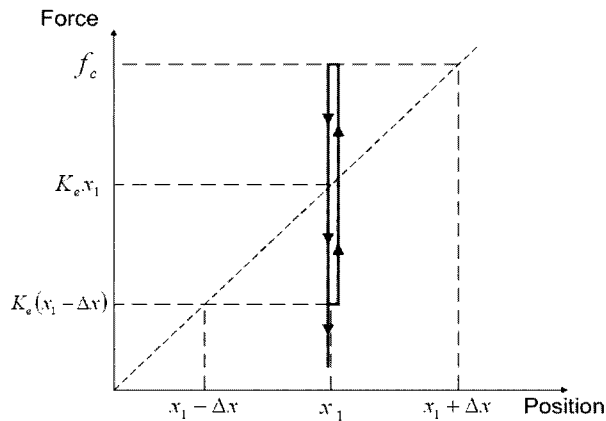


그림 12. 속도의 부호가 한 샘플타임 후에 변할 때, 실제변위에 따른 힘의 변화.

Fig. 12. Actual position vs. force response when the sign of the velocity is suddenly changed in one sample time.

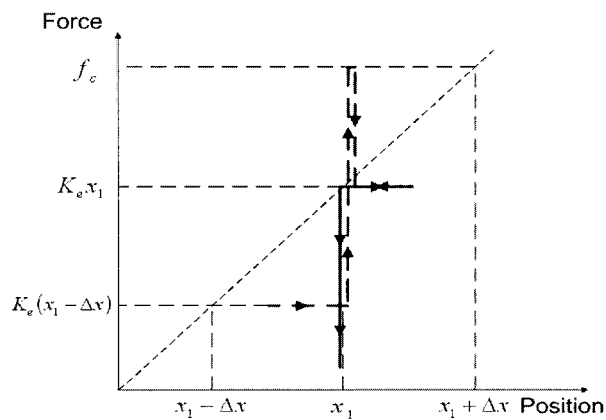


그림 13. 저속구간에서 속도의 부호가 바뀔 때, 실제 변위에 따른 힘의 변화.

Fig. 13. Actual position vs. force response when the sign of the velocity is changed during low velocity.

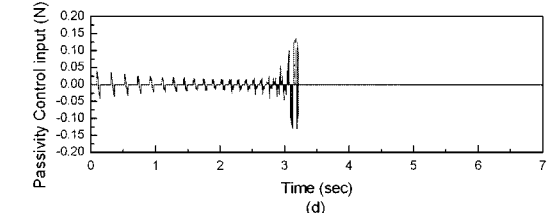
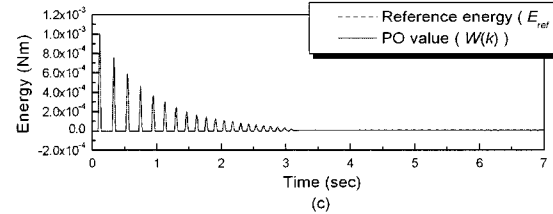
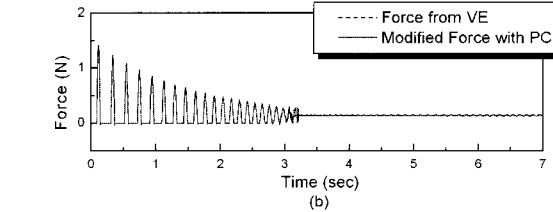
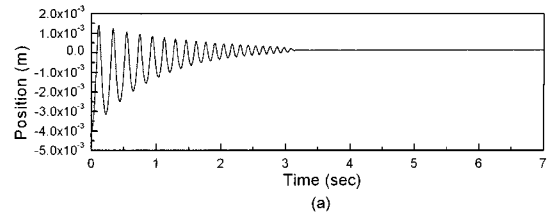


그림 14. 속도부호의 변화에 따른 에너지의 변화를 무시할 경우 접촉응답.

Fig. 14. Contact response with the proposed energy ignoring method from sign change.

Not only sudden sign change but also slow sign change like Fig. 11 could give undesirable effect to the PO value. However this effect is ignorable if the sampling rate is fast enough. Fig. 13 shows different two paths of the actual position vs. force response when it was compressed (dashed line) and released (solid line). Note that one sample time after the actual position crossed x_1 , the output force was decreased to $K_e x_1$ and stayed until the position became less than x_1 . This behavior produced two rectangles. The area of upper one is the dissipated energy with the PC, and the lower one is the produced energy due to the velocity sign change. If the PO value and the reference energy were same at the beginning of this graph, f_c would be same as $K_e(x_1 + \Delta x)$. Please see [18]. Therefore the dissipated and produced energy would be summed to almost zero as long as the actual position is not suddenly changed.

We assume that the inherent dissipative elements in HI and HO are enough to dissipate the produced energy for the above two cases, if there is. As a result, it can be ignorable that the negative effect of the PO value from the above two sign changes.

Fig. 14 shows the result of the simulation which ignores the change of the PO value from the sign change. Noisy behavior

and the PC control force were significantly reduced. However, during the transient time (near $t=3$ (sec)), some levels of noisy behavior remained (Fig. 14b,d). This was because the zero value of the velocity could not contribute to modify the PO value.

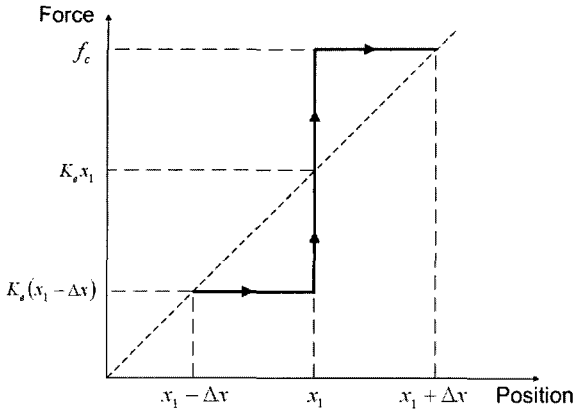


그림 15. 속도가 0인 구간에서 PC입력이 유지될 경우, 실제 변위에 따른 힘의 변화.

Fig. 15. Actual position vs. force response when the PC force is held while the velocity is zero.

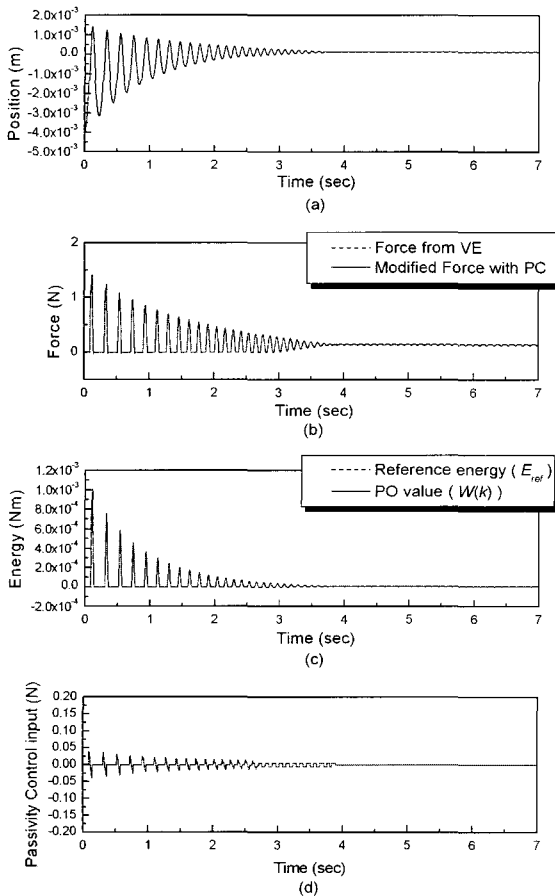


그림 16. PC입력 유지 및 에너지변화 무시방법을 동시에 적용한 경우의 접촉응답.

Fig. 16. Contact response with the PC force holding and the energy ignoring method as well.

2. Holding the PC Force during Zero Velocity

Since we found that the actual velocity was nonzero, even though the numerically calculated velocity was zero, The PC force was held during the zero velocity for using actual velocity information. In Fig. 15, the PC force was held during the measured position was constant. Even though the measured position was constant, the actual position was gradually increased from x_1 to $x_1 + \Delta x$. Therefore, the PC force could contribute to compensate the energy difference. Moreover, once the measured position became greater than or equal to $x_1 + \Delta x$, the compensated energy was automatically updated considering the actual position displacement without any PO modification.

Table 1 summarizes the mentioned overall compensation algorithm of the PO/PC including ignoring the produced energy and holding the PC force schemes, where δ is the minimum resolution of the position sensor, $\Delta x(k) = x(k) - x(k-1)$, and f_{PC} is the PC force.

The proposed holding and ignoring algorithm were implemented to the same simulation as Fig. 14. The noisy behavior during the transient state was removed (Fig. 16b), and the unnecessary PC force was also significantly reduced (Fig. 16d).

V. Experimental Results

The similar experiment with the simulation in Section III and

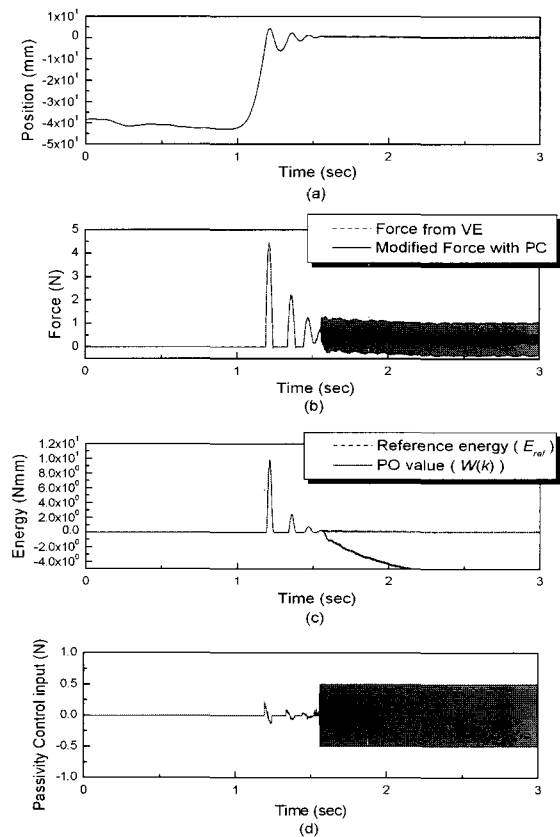


그림 17. 제안된 방법이 사용 안된 기존의 실험결과.

Fig. 17. Experimental result with the PO/PC without the proposed methods.

and IV was done with a PHANTOM haptic device and GHOST SDK. We made a contact with a VE ($K = 1000 \text{ N/m}$) at Position > 0 by applying the previous PO/PC in [18]. The device was pushed to make a contact and operator kept pushing the VE to maintain the contact. Without the proposed methods, the similar result with the simulation (Fig. 3) was obtained. The position response seemed stable (Fig. 17a), but the modified force was vibrating (Fig. 17b), and operator felt small and continuous vibration during the period of low velocity (See Fig. 17).

If the experimental result was magnified, similar trends of the velocity and the PO responses were found, which were the main reasons of the noisy behavior as we found in Fig. 5 and Fig. 8 through the simulation. During $t=1.556 - 1.561$ (sec), the sudden and continuous sign changes of the velocity and its negative effect

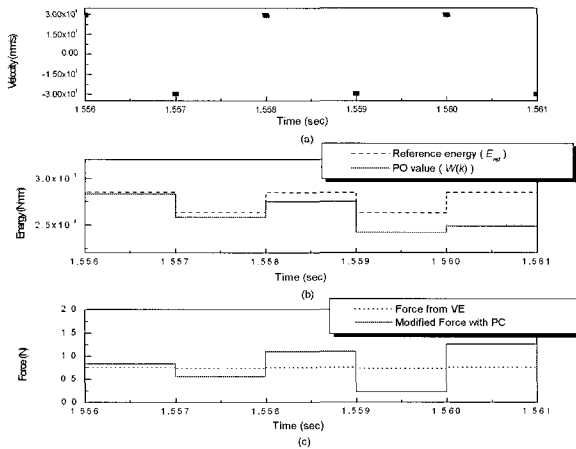


그림 18. 갑작스런 속도의 변화와 그에 의한 PO값의 변화. 시뮬레이션 결과인 그림 5와 비슷한 경향을 가짐. Fig. 18. Sudden sign change of the velocity and its effect to the PO value. experimental results are similar to the simulation results in fig. 5.

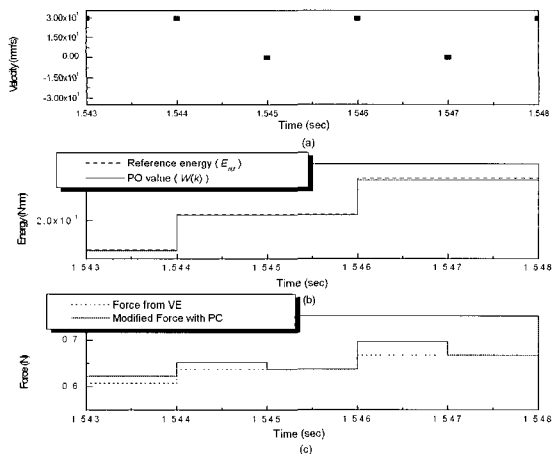


그림 19. PC동작 후 속도가 0이 된 경우, PO값에 미치는 영향. 시뮬레이션 결과인 그림 8과 비슷한 경향을 가짐. Fig. 19. Zero velocity after the PC action and its effect to the PO value. experimental results are similar to the simulation results in fig. 8.

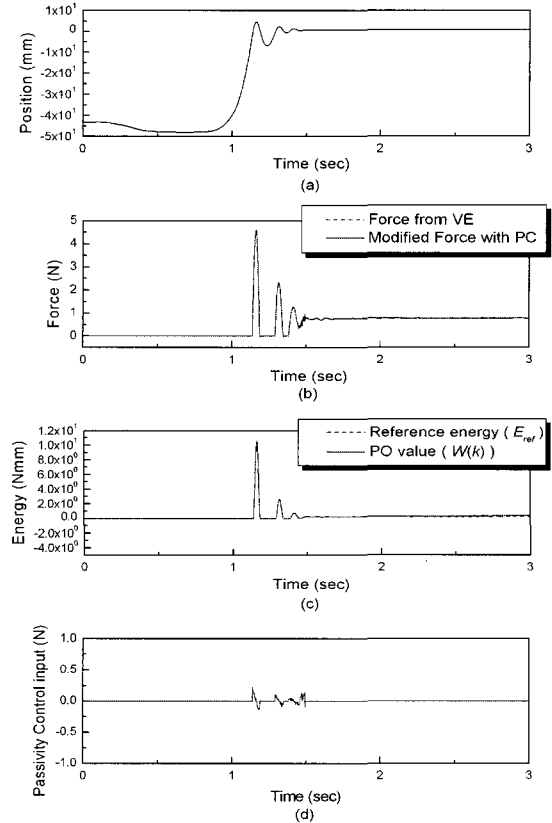


그림 20. 제안된 방법을 사용한 실험결과. Fig. 20. Experimental result with the PO/PC with the proposed methods.

표 1. 잡음을 없애기 위한 향상된 PO/PC 방법.

Table 1. Improved PO/PC algorithm for removing the noisy behavior.

$$\begin{aligned}
 & \text{If } |\Delta x(k)| < \delta \{ \\
 & \quad f_{PC}(k) = f_{PC}(k-1) \\
 & \quad W(k) = W(k-1) + f_c(k-1)\Delta x(k) \\
 & \} \text{ else } \{ \\
 & \quad \text{If } ((\Delta x(k) = -\text{Prev}_{\Delta x}) \& (\Delta x(k) = \delta)) \{ \\
 & \quad \quad W(k) = W(k-1) - \text{Prev}_{f_c} \text{Prev}_{\Delta x} \\
 & \quad \} \text{ else } \{ W(k) = W(k-1) - f_c(k-1)\Delta x(k) \\
 & \quad \} \\
 & \quad \text{Prev}_{\Delta x} = \Delta x(k), \quad \text{Prev}_{f_c} = f_c(k) \\
 & \quad \text{If } (W(k) < E_{ref}(k)) \{ \\
 & \quad \quad f_{PC}(k) = -\frac{W(k) - E_{ref}(k)}{\Delta x(k)} \\
 & \quad \} \text{ else } \{ f_{PC}(k) = 0 \\
 & \quad \} \\
 & \} \\
 & f_{PC}(k) = f_c(k) + f_{PC}(k)
 \end{aligned}$$

to the PO value were found (Fig. 18(a, b, c) like in Fig. 5. Fig. 19(a, b, c) shows the zero values of the velocity after PC action and its effect to the PO value. During $t=1.543 - 1.548$ (sec) the same behavior as in Fig. 8 was found. Therefore, it is reasonable to apply the proposed methods from the simulation

to the experiment for compensating the noisy behavior.

By applying the proposed methods, the noisy behavior was significantly removed, and operator felt smooth force as shown in Fig. 20.

VI. Conclusion and Future Works

In this paper, methods to remove the noisy behavior of the PO/PC are proposed through the deep analysis of the simulation and experiment. There were two main reasons of the noisy behavior. One of them was the sign change of the numerically calculated velocity. This was because we can not help estimating the future velocity for calculating the current PO/PC. The other one was the zero value of the velocity after the PC action. Since the calculated velocity was zero for the most of the time during the period of low velocity even though the actual velocity was not, the PO became conservative and generated the nonnecessary PC force. The method for solving the first problem was ignoring the difference of the PO value from the velocity sign change based on the assumption that the actual energy difference is significantly small and can be dissipatable with the inherent damping of HO and HI. The other method for solving the second problem was holding the PC force during zero velocity since the actual velocity is not zero. The feasibility of the proposed methods was proved through the simulation and the experiment, and the PO/PC approach became more practical with the proposed methods.

In some case, the produced energy from the velocity sign change may not be ignorable. If the sampling rate is not fast enough compared to the system mode, the position sensor can not catch the exact instance when the actual position crosses the digitized line. As a result, the width of the rectangle in Fig. 12 will be increased, and the amount of the produced energy may become greater than the allowable energy. Therefore, it is better to turn off the PC when the velocity sign change is repeated. To find the exact condition when the PO/PC is not effective anymore, we are studying the limitation of the PO/PC approach as a further work.

References

- [1] R. J. Adams and B. Hannaford, "Stable haptic interaction with virtual environments," *IEEE Trans. on Robotics and Automation*, vol. 15, no. 3, pp. 465-474, 1999.
- [2] R. J. Anderson and M. W. Spong, "Asymptotic stability for force reflecting teleoperators with time delay," *Int. Journal of Robotics Research*, vol. 11, no. 2, pp. 135-149, 1992.
- [3] F. Barbagli, D. Prattichizzo and K. Salisbury, "Multirate analysis of haptic interaction stability with deformable objects," *IEEE Int. Conf. on Decision and Control*, Italy, 2002, pp. 917-922.
- [4] J. E. Colgate, and J. M. Brown, "Factors affecting the z-width of a haptic display," *Proc. IEEE Int. Conf. Robot. Automat.*, San Diego, CA, May 1994, pp. 3205-3210.
- [5] J. E. Colgate, and G. Schenkel, "Passivity of a class of sampled data systems: application to haptic interfaces," *American Control Conference*, Baltimore, MD, 1994, pp. 3236-3240.
- [6] B. Hannaford, and J. H. Ryu, "Time domain passivity control of haptic interfaces," *IEEE Trans. on Robotics and Automation*, vol. 18, no. 1, pp. 1-10, 2002.
- [7] F. Janabi-Sharifi, V. Hayward, and C.-S. J. Chen, "Discrete-time adaptive windowing for velocity estimation," *IEEE Trans. on Control Systems Technology*, vol. 8, no. 6, pp. 1003-1009, 2000.
- [8] Y. S. Kim and B. Hannaford, "Some practical issues in time domain passivity control of haptic interfaces," *Proc. IEEE/RSJ Int. Conf. on Intelligent Robotics and Systems*, Maui, Hawaii, 2001, pp. 1744-1750.
- [9] B. Kumar, and S. C. Dutta Roy, "Design of digital differentiators for low frequencies," *Proc. IEEE*, vol. 76, pp. 287-289, Mar. 1988.
- [10] D. Lee, and P. Y. Li, "Towards robust passivity: A passive control implementation structure for mechanical teleoperators," *11th Haptics and Teleoperator Symposium*, Los Angeles, March 2003, pp. 132-139.
- [11] S. Mahapatra, and M. Zefran, "Stable haptic interaction with switched virtual environments," *Proc. IEEE Int. Conf. Robot. Automation*. Taipei, Taiwan, 2003, pp. 14-19.
- [12] D. T. McRuer, "Human dynamics in man-machine systems," *Automatica*, vol. 16, no. 3, pp. 237-253, 1980.
- [13] D. T. McRuer, and E. S. Krendel, "The human operator as a servo element," *J. Franklin Inst.*, vol. 267, pp. 381-403, 1959.
- [14] B. E. Miller, J. E. Colgate and R. A. Freeman, "Environment delay in haptic systems," *Proc. IEEE Int. Conf. Robot. Automat.*, San Francisco, CA, April, 2000, pp. 2434-2439.
- [15] G. Niemeyer and J. J. Slotine, "Stable adaptive teleoperation," *IEEE Journal of Oceanic Engineering*, vol. 16, pp. 152-162, 1991.
- [16] J. H. Ryu, D. S. Kwon and B. Hannaford, "Stable teleoperation with time domain passivity control," *IEEE Trans. on Robotics and Automation*, vol. 20, no. 2, pp. 365-373, 2004.
- [17] J. H. Ryu, Y. S. Kim, and B. Hannaford, "Sampled and continuous time passivity and stability of virtual environments," *IEEE Trans. on Robotics*, vol. 20, no. 4, pp. 772-776, 2004.
- [18] J. H. Ryu, B. Hannaford, C. Preusche, and G. Hirzinger "Time domain passivity control with reference energy behavior," *Proc. IEEE/RSJ Int. Conf. on Intelligent Robotics and Systems*, Las Vegas, USA, 2003, pp. 2932-2937.
- [19] S. Stramigioli, C. Secchi and A. J. van der Schaft, "A novel theory for sampled data system passivity," *IEEE/RSJ Int. Conf. on Intelligent Robotics and Systems*, Switzerland, 2002, pp. 1936-1941.
- [20] A. J. van der Schaft, "L2-gain and passivity techniques in nonlinear control," *Springer, Communications and Control Engineering Series*, 2000.
- [21] J. C. Willems, "Dissipative dynamical systems, part I: General theory," *Arch. Rat. Mech. An.*, vol. 45, pp. 321-351, 1972.
- [22] C. B. Zilles and J. K. Salisbury, "A constraint-based god-object method for haptic display," *Proc. IEEE/RSJ Int. Conf. on Intelligent Robotics and Systems*, Pittsburgh, PA, 1995, pp. 146-151.



유지환

2002년 한국과학기술원 기계공학과 박사 졸업. 2002년~2003년 미국 University of Washington 전자공학과 Post Doc. 2003년~2005년 KAIST 전기 및 전자공학과 연구교수. 2005년~현재 한국기술교육대학교 기계정보공학부 전임강사.